

PACS numbers: 42.30.Wb; 87.64.Cc; 05.10.Ln
DOI: 10.1070/QE2006v036n12ABEH013457

Simulations of a spatially resolved reflectometry signal from a highly scattering three-layer medium applied to the problem of glucose sensing in human skin

A.V. Bykov, M.Yu. Kirillin, A.V. Priezzhev, R. Myllylä

Abstract. **The possibility of using spatially resolved reflectometry (SRR) at a wavelength of 820 nm to detect changes in the optical properties of a highly scattering layered random medium simulating a biological tissue caused by changes in the glucose level is analysed. Model signals from a three-layer biological tissue phantom consisting of two skin layers and a blood layer located between them are obtained by the Monte-Carlo method. It was assumed that variations in the glucose level induce variations in the optical parameters of the blood layer and the bottom skin layer. To analyse the trajectories of photons forming the SRR signal, their scattering maps are obtained. The ratio of the photon path in layers sensitive to the glucose level to the total path in the medium was used as a parameter characterising these trajectories. The relative change in the reflected signal caused by a change in the glucose concentration is analysed depending on the distance between a probe radiation source and a detector. It is shown that the maximum relative change in the signal (about 7 %) takes place for the source – detector separation in the range from 0.3 to 0.5 mm depending on the model parameters.**

Keywords: *spatially resolved reflectometry, near-IR range, optics of biological tissues, glucose level, Monte-Carlo method.*

A.V. Bykov Department of Physics, International Laser Center, M.V. Lomonosov Moscow State University, Vorob'evy gory, 119992 Moscow, Russia; present address: Department of Electrical and Information Engineering, Optoelectronics and Measurement Techniques Laboratory, University of Oulu, P.O. Box 4500, 90014 University of Oulu, Finland; e-mail: sasha5000@tut.by;
M.Yu. Kirillin Department of Physics, M.V. Lomonosov Moscow State University, Vorob'evy gory, 119992 Moscow, Russia; present address: Department of Electrical and Information Engineering, Optoelectronics and Measurement Techniques Laboratory, University of Oulu, P.O. Box 4500, 90014 University of Oulu, Finland; e-mail: mkirillin@yandex.ru;
A.V. Priezzhev Department of Physics, International Laser Center, M.V. Lomonosov Moscow State University, Vorob'evy gory, 119992 Moscow, Russia; e-mail: avp2@mail.ru, avp2@phys.msu.ru;
R. Myllylä Department of Electrical and Information Engineering, Optoelectronics and Measurement Techniques Laboratory, University of Oulu, P.O. Box 4500, 90014 University of Oulu, Finland; e-mail: risto.myllyla@ee.oulu.fi

Received 10 August 2006
Kvantovaya Elektronika **36** (12) 1125 – 1130 (2006)
Translated by M.N. Sapozhnikov

1. Introduction

At present the development of new methods for measuring and monitoring the glucose level in human tissues is an urgent problem of biomedical diagnostics, which is related to the widespread incidence of diabetes (over 170 million people over the world [1]). Among the methods being developed, the most promising are noninvasive methods, which do not require the sampling of blood from patients for analysis and provide the continuous control (monitoring) of the glucose level in blood. In this connection, different optical methods were tested for their sensitivity to measure the glucose level in human tissues [2].

Laser methods for measuring the glucose level in blood and liquids in tissues are based on the fact that a change in the glucose content induces a change in the optical properties of a scattering medium, in particular, its scattering coefficient μ_s and the effective anisotropy factor g. This occurs due to a change in the refractive index n of the medium surrounding light-scattering particles (cells) (in the case of blood, this medium is blood plasma) [3], which in turn results in changes in the average scattering cross section and the shape of the scattering phase function of particles. It was shown in papers [4 – 6] that the presence of glucose in a scattering random medium changes its parameters in the following way:

$$n = n^0 + 1.515 \times 10^{-6} C, \tag{1}$$

$$\mu_s = (1 - 2.2 \times 10^{-4} C/18)\mu_s^0, \tag{2}$$

$$g = (1 + 7 \times 10^{-6} C/18) g^0, \tag{3}$$

where C is the glucose concentration in mg dL^{-1}; n, μ_s, g, and n^0, μ_s^0, g^0 are the refractive index, scattering coefficient, and anisotropy factor of the medium after and before the addition of glucose to the medium, respectively.

It was proposed recently [7 – 9, 10] to use optical coherence tomography and time-of-flight photometry for measuring and monitoring the glucose level in scattering media. We suppose that it is also expedient to study the sensitivity of spatially resolved reflectometry (SRR), which has been efficiently applied for measuring the oxygenation level of haemoglobin in human blood [11], to a change in the glucose level in human tissues. The efficiency of this method for measuring the glucose level in blood was demonstrated earlier in [12].

The aim of this paper is the numerical Monte-Carlo (MC) study of the possibility of using SRR for noninvasive measurements of variations in the glucose level in a highly scattering layered random medium by the example of the three-layer model of skin containing a blood layer and also the determination of the optimal detection parameters.

2. Monte-Carlo simulations of SRR signals

The Monte-Carlo method is based on the procedure of statistical tests. Monte-Carlo simulations of radiation propagation in a scattering medium involve repeated calculations of random photon trajectories and a subsequent analysis of accumulated statistical data. In this paper, we used the program realisation of the MC method that we developed earlier [11, 13–15] to simulate signals obtained by different optical diagnostic methods, including SRR. The SRR method is based on the measurement of the radiation intensity I backscattered by a medium as a function of the distance r between a light source and a detector. This dependence is called a SRR signal. Such measurements are usually performed by using a linear detector array placed on the same surface of the medium as the source or by displacing one detector by steps along some line. As a rule, fibreoptic detectors are used in modern setups, so that a measuring head directly adjacent to the object under study consists of a set of optical fibres of a chosen diameter with the specified numerical aperture.

The statistical averaging in the MC method is performed over detected photons. To increase the number of detected photons, we assumed in our calculations that the number of emitted photons was 10^9. To accelerate MC simulations in the case of an axially symmetric medium, the distribution of a signal depending on the source–detector separation is usually calculated not along one chosen direction but in all directions, which gives after normalisation the result based on a larger statistics.

3. Multilayer biological tissue model

The results of MC simulations of radiation propagation in biological tissues or model media depend to a great extent on the choice of the model of the object under study and its optical parameters. Because optical parameters of different biological tissues (absorption and scattering coefficients, and the anisotropy factor) are measured indirectly [16], their values determined by different authors differ strongly depending on the sample type and the calculation method. For example, it was shown in [17] that, depending on the form of the scattering phase function of a particle, the calculated optical parameters of the medium can change by an order of magnitude.

Various optical methods and MC simulations are often tested by using the aqueous solution of intralipid whose optical properties at the concentration 2 % are close to those of skin [18]. Intralipid is a polydisperse suspension of nearly spherical scattering particles of average diameter about 0.3 μm suspended at concentrations 10 % or 20 % in the glycerol-water mixture. The scattering particles are drops of soybean oil covered with a thin lipid membrane of thickness 2.5–5.0 nm [19, 20]. However, a comparison between the optical properties of skin and intralipid solution shows that the anisotropy factors of these two media are different, although the reduced scattering coefficients $\mu_s' = (1-g)\mu_s$ can be close. For this reason, we considered here a three-layer model consisting of two layers, characterised by the averaged optical parameters of skin, and a layer located between them and characterised by blood parameters. It was assumed in simulations that a change in the glucose concentration does not change the optical properties of the upper skin layer because the glucose level in the human organism changes first in blood and then in tissues adjacent to blood vessels, while variations in the glucose level in the surface skin layer occur later and they are insignificant.

The scheme of the simulated experiments is presented in Fig. 1. The embedment depth L_1 of the blood layer was varied from 100 to 300 μm, which corresponds to the range of embedment depths of the upper capillary plexus of human skin. The thickness L_2 of the blood layer was fixed at 200 μm. The thickness of the lower skin layer was chosen to obtain the total thickness of a sample equal to 10 mm. This thickness is large enough to consider the lower layer as semi-infinite.

The normal glucose level in human blood lies in the range from 70 to 160 mg dL^{-1} [2]. In this paper, we considered variations in the glucose level from 0 to 500 mg dL^{-1}, which covers the range of physiological glucose concentrations in blood, the extreme values of this range corresponding to pathological cases.

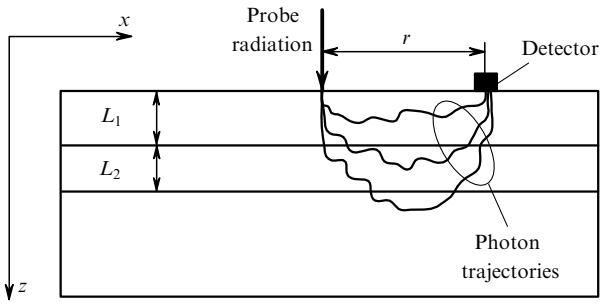

Figure 1. Scheme of the simulated experiment.

Optical parameters characterising the layers simulating skin were averaged by using their values presented in [16, 21, 22], whereas for a layer simulating blood they were taken from [23]. These parameters are presented in Table 1. The probe radiation wavelength was set equal to 820 nm because this wavelength lies within the so-called diagnostic transparency window (600–1300 nm) and is widely used in the noninvasive diagnostics of biological tissues.

Table 1. Optical parameters used in simulations ($\lambda = 820$ nm).

Medium	μ_s/mm^{-1}	μ_a/mm^{-1}	g	n	l_{tr}/mm
Blood	57.3	0.82	0.977	1.4	0.468
Skin	10	0.002	0.9	1.4	0.98
Intralipid	10	0.002	0.7	1.4	0.33

We used in simulations two values of the anisotropy factor typical for skin (0.9) and the aqueous solution of intralipid (0.7). Because this factor plays a considerable role in the propagation of light in a scattering medium, it is important to analyse its influence on the results. Table 1 also

presents the transport length $l_{tr} = (\mu_a + \mu'_s)^{-1}$ for both media (where μ_a is the absorption coefficient of a medium). This parameter characterises the photon free path in a medium after which the direction of its propagation becomes random.

4. Results and discussion

4.1 SRR signals

The SRR signals were calculated as a function of the source–detector separation r for the above-described model (phantom) of a biological tissue by the MC method and the discrete-coordinate grid method by using the RADUGA-5.1(P) program [24]. These dependences obtained for the zero concentration of glucose are presented in Fig. 2. Good agreement between the results obtained by these two methods suggests that they are adequate. Signals obtained by the MC method for a medium simulating skin for $g = 0.9$, the blood embedment depth 200 μm, and glucose concentrations 0 and 500 mg dL^{-1} are presented in the interval of their maximum difference in the inset in Fig. 2.

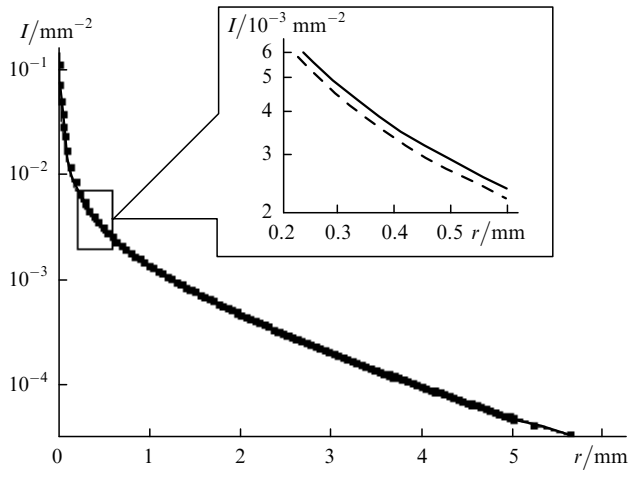

Figure 2. Spatially resolved reflectometry signals from a three-layer medium for the embedment depth of the second layer simulating blood $L_1 = 200$ μm and the zero glucose concentration obtained by the discrete-coordinate (■) and MC (solid curve) methods. The inset shows signals obtained by the MC method for the glucose concentration equal to 0 (solid curve) and 500 mg dL^{-1} (dashed curve) for the skin anisotropy factor $g = 0.9$ in the interval of the maximum relative difference of the signals.

The dependences of the number of detected photons on the source–detector separation are normalised to the detector area and the total number of emitted probe photons. The numerical aperture of the detector was set equal to NA = 0.24, which corresponds to the receiving cone angle of 28°. Thus, the dimensionality of the quantity I in Fig. 2 is mm^{-2}. The reflection coefficient R of the detector surface, which was calculated by using Fresnel formulas, is ~ 1 %. Therefore, this reflection was neglected in calculations. However, it can be further decreased by filling the space between the detector and sample by an immersion liquid.

The detected radiation power P can be calculated from the dependences presented in Fig. 2 by the expression

$$P = P_0(1 - R)IS_d,$$

where P_0 is the probe radiation power and S_d is the detector area. Of course, the calculation by this expression is correct only if the linear size of the detector is smaller than the characteristic distance at which the SRR signal changes considerably.

An important parameter of measurements is the probe radiation intensity. In the case of glucose detection, the probe radiation intensity is strictly limited because the heating of a tissue even by 1 °C can induce changes in the optical properties resulting in the error in the measurement of the glucose level [6]. Therefore, according to the data presented in [14], the maximum intensity in this case is ~ 1 W mm^{-2}.

The spatial resolution in the calculation of the SRR signal was 20 μm, which corresponds in principle to the linear size of the detector (or the diameter of an optical fibre directed to the detector). This means that in this case the detector area is ~ 400 μm^2, the detected power is $10^{-4} - 10^{-8}$ W, and the corresponding intensities are $10^{-1} - 10^{-5}$ W mm^{-2} for source–detector separations $r = 0 - 8$ mm and the maximum probe radiation intensity. This radiation power can be measured quite accurately with modern detectors. The power of a detected signal can be obviously increased by increasing the detector area because the chosen value 20 μm is a model parameter rather than the real diameter of a fibre.

4.2 Relative sensitivity of the SRR method

We estimated the relative sensitivity S of the SRR signal to variations in the glucose concentration depending on the source–detector separation r from the expression

$$S(r) = \left| \frac{I_0(r) - I_{500}(r)}{I_0(r)} \right|,$$

where I_0 and I_{500} are SRR signals at glucose concentrations 0 and 500 mg dL^{-1}. The results obtained for three embedment depths of the blood layer are presented in Fig. 3. The signal fluctuations at large distances r are the result of insufficient statistics. One can see that for $g = 0.9$ (Fig. 3a), the relative sensitivity S has a local maximum at $r \approx 0.4$ mm. The minimum at $r \approx 2.5$ mm appears because the difference $I_0(r) - I_{500}(r)$ changes its sign, and since the quantity S is introduced as nonnegative, it has the minimum for $I_0(r) - I_{500}(r) = 0$. The sensitivity S again achieves a local minimum at the distance $r \approx 7$ mm. In this case, the power of detected radiation decreases by three orders of magnitude compared to its value for $r = 0.4$ mm, i.e. it is better, of course, to perform measurements for $r = 0.4$ mm. Moreover, as will be shown below, photons forming a backscattered signal at $r = 7$ mm achieve the penetration depth in the medium comparable with r. However, the thickness of human skin is only 2–3 mm, although we considered the sample of a greater thickness in our model.

For $g = 0.7$ (Fig. 3b), the relative sensitivity S also has a maximum at $r \approx 0.5$ mm. However, Fig. 3b shows that in this case the position and intensity of the maximum stronger depends on the embedment depth of the blood layer. In addition, the value of S for small r is lower than in the case of $g = 0.9$, which is related to a greater stochastisation of the propagation direction of a photon before it reaches 'glucose-

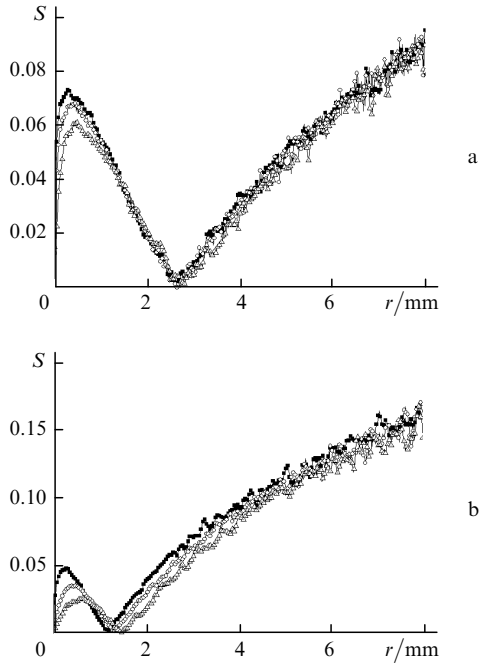

Figure 3. Relative sensitivity S of the SRR signal to the change in the glucose concentration from 0 to 500 mg dL^{-1} in the blood layer and depth skin layer for $L_1 = 100$ (■), 200 (○), and 300 μm (△) and the skin anisotropy factor $g = 0.9$ (a) and 0.7 (b).

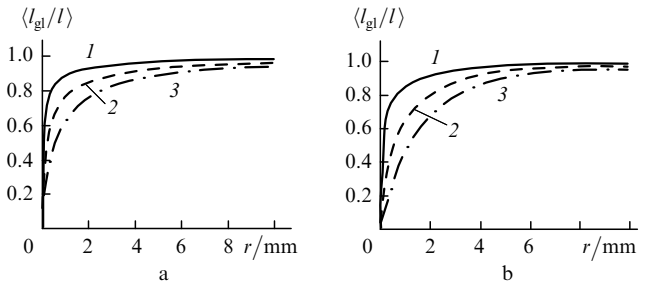

Figure 4. Mean ratio of the photon free path l_{gl} in layers with optical characteristics dependent on the glucose concentration to the total photon path l in the medium for $L_1 = 100$ (*1*), 200 (*2*), and 300 μm (*3*) for the skin anisotropy factor $g = 0.9$ (a) and 0.7 (b).

sensitive' layers, i.e. layers whose optical characteristics are sensitive to variations in the glucose concentration. Thus, while for $g = 0.9$ the transport length considerably exceeds the embedment depth of blood layers, for $g = 0.7$ it is equal to 0.33 mm (see Table 1), which is comparable to the embedment depth of the blood layer. Therefore, in the case of the maximum considered embedment depth of the blood layer, the regime is realised in fact when the propagation direction of a photon becomes stochastic before it reaches 'glucose-sensitive' layers. In this case, the 'sensitivity' to glucose is observed at large distances r, where diffusion backscattering is realised.

4.3 Information content of a single photon

The sensitivity of the SRR method analysed by using MC simulations is determined by two quantities; the number of photons contributing to a signal and the mean sensitivity of a single photon (i.e. by some averaged photon characteristic dependent on the optical properties of the medium). In the SRR method, this characteristic is the photon trajectory which depends on the structure and optical properties of the medium. The results of this analysis can be extended to real experimental conditions.

In the case under study, the decisive factor is the propagation of a photon in layers whose optical characteristics depend on the glucose concentration (blood and depth skin layers). We characterised the information content of a photon by the ratio of the photon free path in these layers to its total path in the medium. The dependences of this characteristic on the source–detector separation obtained for different parameters of the medium are presented in Fig. 4. One can see that the information content of a photon monotonically increases with increasing the source–detector separation. This is explained by the fact that, as the source–detector separation is increased, the fraction of the photon path in the upper layer where the influence of glucose is absent decreases. The same tendency takes place with decreasing the upper layer thickness, which results in an increase in the photon sensitivity at fixed r with decreasing the upper layer thickness.

Note also that the increase in the information content of a single photon with depth is compensated by a drastic decrease in the signal intensity, so that the distance $r = 0.4$ mm should be considered optimal for the model under study. Moreover, the detected power for this source–detector separation is not so small ($\sim 10^{-6}$ W) as for $r = 7$ mm ($\sim 10^{-8}$ W), which imposes milder requirements on the detector sensitivity.

4.4 Scattering maps

To analyse the trajectories of photons forming the SRR signal, we obtained scattering maps characterising the density of scattering events in the medium. The brightness at each point of the map is proportional to the number of scattering events. The scattering maps were obtained for the blood embedment depth $L_1 = 200$ μm and distances $r = 400$, 800, and 1200 μm. The results are presented in Fig. 5. The scattering maps illustrate the distribution of trajectories with a high density and small width at the points of radiation coupling and detection. The distribution between these points has a low density and broadens. The density of trajectories is proportional to the picture brightness, which is much higher in the region corresponding to the blood layer because the map is the density of scattering events of photons forming the signal, and the scattering coefficient of blood exceeds that of skin approximately by a factor of five.

The trajectory distributions for $g = 0.9$ are narrower than those for $g = 0.7$, which is explained by a greater chaotisation of photon propagation directions in the latter case. As the source–detector separation is increased, the overlap of the brightest parts of the picture in the embedment regions of the source and detector decreases.

The information content of a photon should increase with increasing the photon path in layers 'sensitive' to the glucose concentration. Therefore, it is reasonable to expect that the photon information content will be maximal when the photon path in the upper layer is minimal (i.e. when photons intersect this layer almost perpendicular), which is realised with a higher probability for $g = 0.9$. This fact is also confirmed in Fig. 3.

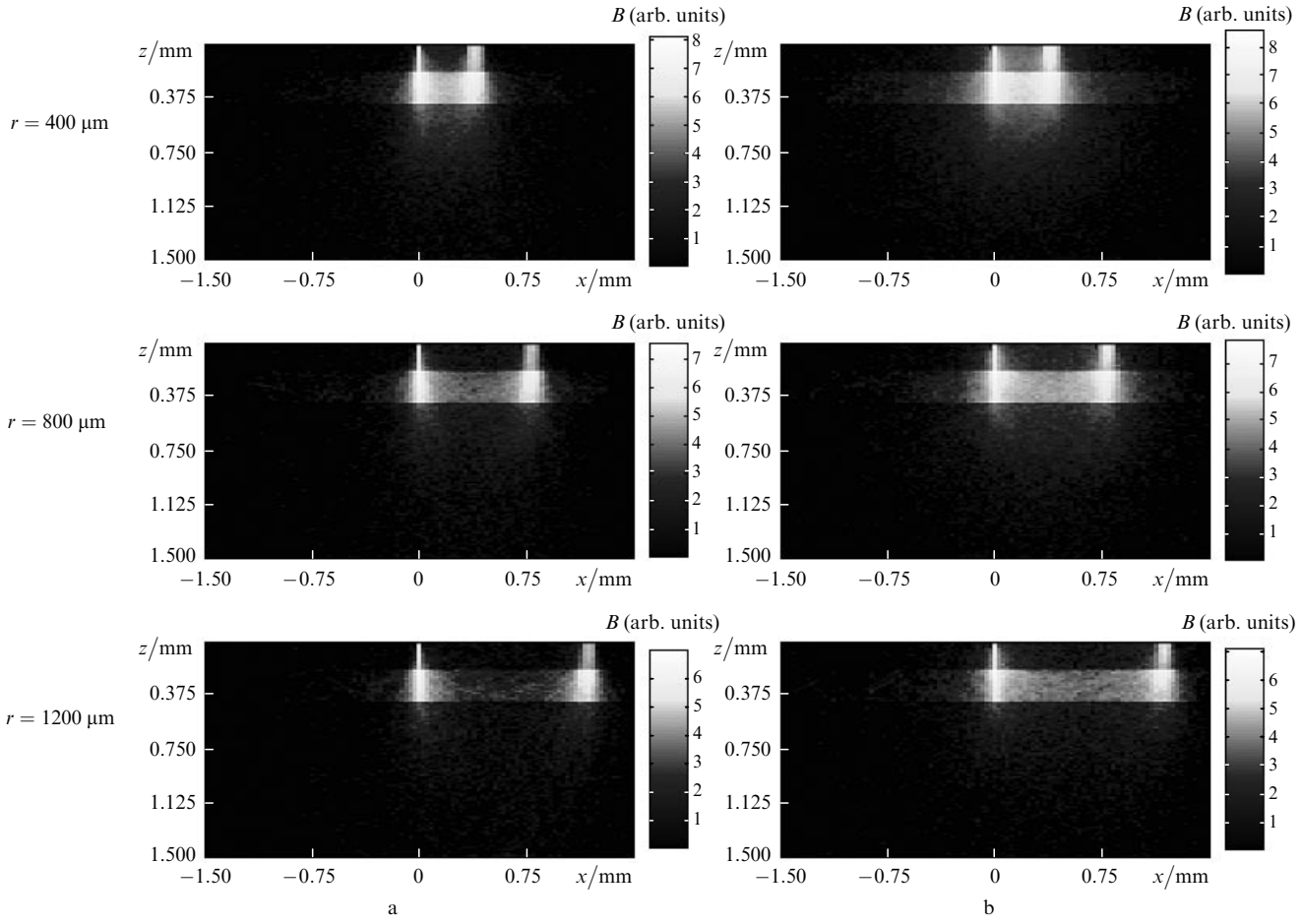

Figure 5. Scattering maps of photons forming the SRR signal in a three-layer skin model for $L_1 = 200$ μm, the skin anisotropy factor $g = 0.9$ (a) and 0.7 (b), and different distances r. The coordinate origin coincides with the point of incidence of probe radiation.

4.5 Dependence of the SRR signal on the glucose concentration

At the final stage of the study, we investigated the dependence of the SRR signal on the glucose concentration for the blood embedment depth 100 μm for the two combinations of parameters: $g = 0.9$, $r = 0.4$ mm and $g = 0.7$, $r = 0.3$ mm. As shown above, these combinations of parameters are optimal. The results are presented in Figs 6a and b, respectively. One can see that a distinct correlation is observed between the detected SRR signal and glucose concentration in the medium in the range from 0 to 500 mg dL^{-1}.

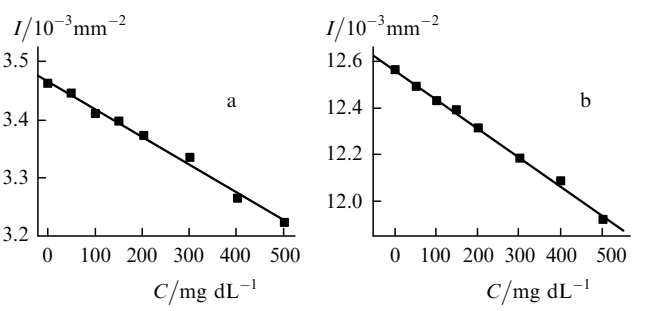

Figure 6. Dependences of the SRR signal for $g = 0.9$, $r = 0.4$ mm (a), and $g = 0.7$, $r = 0.3$ mm (b) on the glucose concentration C in depth layers of the phantom for $L_1 = 100$ μm.

If the above-mentioned optical fibre with a cross-sectional area of ~ 400 μm^2 is used, the detected power will be from 1.28 to 1.4 μW upon changing the glucose concentration from 0 to 500 mg dL^{-1}, which will require, of course, a high enough detection accuracy. However, the cross-sectional area of the optical fibre presented above is a characteristic of the method used rather than the real characteristic of a measuring system. Of course, the detected power will increase with increasing the fibre diameter, which will reduce the requirements on the sensitivity of a photodetector. Thus, the sensitivity of a ThorLabs APD210 photodetector in the wavelength region that we consider is 10^5 V W^{-1}, which is sufficient for reliable measurements of signals for the cross-sectional area of the fibre ~ 0.01 mm^2. In this case, the signal power will vary from 32.1 to 34.7 μW, which will result in the change in the measured voltage from 3.21 to 3.47 V. Therefore, the sensitivity to variations in the glucose concentration will be 0.52 mV mg^{-1}dL.

5. Conclusions

We have analysed the possibility of applications of SRR for the noninvasive detection of the glucose level in the three-layer phantom of human skin. The sensitivity of this method has been estimated for different source–detector separations and different embedment depths of layers containing glucose. It has been shown that the maximum

sensitivity to variations in the glucose concentration in the three-layer model considered in the paper is observed for the source–detector separation equal to 0.4 mm. In this case, the change in the glucose concentration from 0 to 500 mg dL^{-1} results in the change in the detected signal intensity by $\sim 7\,\%$ and the signal power is $\sim 1\,\mu W$ (corresponding to the intensity ~ 10 mW mm^{-2}) for the probe radiation intensity of ~ 1 W mm^{-2}.

We have also obtained the scattering maps for probe radiation upon the formation of SRR signals and have analysed the information content of photons. It has been shown that the mean information content of a single photon monotonically increases with increasing the source–detector separation; however, the detected signal power decreased from 10^2 to $10^{-2}\,\mu W$ (and the corresponding intensity decreased from 0.1 to 10^{-5} W mm^{-2}) with increasing the source–detector separation from 0 to 8 mm. We have found that the sensitivity of the method for the case under study was 0.52 mV mg^{-1} dL.

The results obtained in the paper show that the SRR is promising for detecting variations in the glucose level in human skin models. However, to analyse the sensitivity of the method in *in vivo* measurements, additional investigations are required which would more accurately consider variations in the optical properties of skin induced by various components of blood and intercellular liquid, which were ignored in our model.

Acknowledgements. The authors thank researchers L.P. Bass, O.V. Nikolaeva, and V.S. Kuznetsov at M.V. Keldysh Institute of Applied Mathematics, RAS for performing discrete-ordinate calculations and useful discussions. This work was supported by the Graduate School in Electronics, Telecommunications and Automation (GETA, Finland), Infotech Oulu (Finland), and the Russian Foundation for Basic Research (Grant No. 06-02-17015).

References

1. http://www.who.int/inf-fs/en/fact138.html.
2. McNichols R.J., Coté G.L. *J. Biomed. Opt.*, **5**, 5 (2000).
3. Lopatin V.N., Priezzhev A.V., Aponasenko A.D., et al. *Metody svetorasseyaniya v analize dispersnykh biologicheskikh sred* (Light Scattering Methods in the Analysis of Disperse Biological Media) (Moscow: Fizmatlit, 2004).
4. Larin K.V., Motamedi M., Ashitkov T.V., Esenaliev R.O. *Phys. Med. Biol.*, **48**, 1371 (2003).
5. Maier J.S., Walker S.A., Fantini S., Franceschini M.A., Gratton E. *Opt. Lett.*, **19**, 2062 (1994).
6. Tarumi M., Shimada M., Mukarami T., Tamura M., Arimoto H., Yamada Y. *Phys. Med. Biol.*, **48**, 2373 (2003).
7. Larin K.V., Eledrisi M.S., Motamedi M., Esenaliev R.O. *Diabetes Care*, **25**, 2263 (2002).
8. Larin K., Larina I., Motamedi M., Gelikonov V., Esenaliev R. *Proc. SPIE Int. Soc. Opt. Eng.*, **4263**, 83 (2001).
9. Popov A.P., Priezzhev A.V., Myllylä R. *Kvantovaya Elektron.*, **35**, 1075 (2005) [*Quantum Electron.,* **35**, 1075 (2005).
10. Kinnunen M., Myllylä R., Jokela T., Vainio S. *Appl. Opt.*, **45**, 2251 (2006).
11. Kirillin M.Yu., Priezzhev A.V., Myllylä R. *Proc. SPIE Int. Soc. Opt. Eng.*, **6163**, 6163-25 (2006).
12. Bruulsema J.T., Hayward J.T., Farrell T.J., Patterson M.S., Heinemann L., Berger M., Koschinsky T., Sandahl-Crisniansen J., Orskov H., Essenpreis M., Schmelzeisen-Redeker G., Boecker D. *Opt. Lett.*, **22**, 190 (1997).
13. Kirillin M.Yu., Priezzhev A.V. *Kvantovaya Elektron.*, **32**, 883 (2002) [*Quantum Electron.*, **32**, 883 (2002)].
14. Bykov A.V., Kirillin M.Yu., Priezzhev A.V. *Opt. Spektr.*, **101**, 37 (2006).
15. Kirillin M.Yu., Meglinski I.V., Priezzhev A.V. *Kvantovaya Elektron.*, **36**, 247 (2006) [*Quantum Electron.*, **36**, 247 (2006)].
16. Tuchin V.V. *Lazery i volokonnaya optika v biomeditsinskikh issledovaniyakh* (Lasers and Fibre Optics in Biomedical Studies) (Saratov: Saratov University, 1998).
17. Yaroslavsky A.N., Yaroslavsky I.V., Goldbach T., Schwarzmaier H.J. *J. Biomed. Opt.*, **4**, 47 (1999).
18. Troy T.L., Thennadil S.N. *J. Biomed. Opt.*, **6**, 167 (2001).
19. Flock S.T. et al. *Lasers Surg. Med.*, **12**, 510 (1992).
20. Van Staveren H.J. et al. *Appl. Opt.,* **30**, 4507 (1991).
21. Knuttel A., Boehlau-Godau M. *J. Biomed. Opt.*, **5**, 83 (2000).
22. Meglinski I.V., Matcher S.J. *Med. Biol. Eng. Comp.*, **39**, 34 (2001).
23. Roggan A., Friebel M., Dorshel K., Hahn A., Muller G. *J. Biomed. Opt.*, **4**, 36 (1999).
24. Bass L.P., Nikolaeva O.V., Kuznetsov V.S., Bykov A.V., Priezzhev A.V., Dergachev A.A. *Matem. Model.*, **18**, 29 (2006).